JOURNAL OF MATERIALS SCIENCE 25 (1990) 1305–1312

Combustion synthesis of fine-particle metal aluminates

J. J. KINGSLEY, K. SURESH, K. C. PATIL
Department of Inorganic and Physical Chemistry, Indian Institute of Science, Bangalore 560 012, India

Fine-particle metal aluminates, MAl_2O_4 where M = Mg, Ca, Sr, Ba, Mn, Co, Ni, Cu and Zn as well as $3CaO \cdot Al_2O_3$ (C_3A), $CaAl_{12}O_{19}$ (CA_6) and $MgCeAl_{11}O_{19}$ have been prepared by the combustion of mixtures of the respective metal nitrates (oxidizers) and urea or carbohydrazide (fuels) at 500 or 350° C, respectively, over a time of 5 min. The solid combustion products were identified by their characteristic X-ray powder diffraction patterns. The fine-particle nature of these metal aluminates was investigated using SEM, TEM, particle size analysis and surface area measurements. The surface areas of the as-prepared metal aluminates using carbohydrazide fuel were higher (45 to 85 $m^2 g^{-1}$) compared with urea (1 to 20 $m^2 g^{-1}$).

1. Introduction

Metal aluminates are of interest due to their technological applications as refractories ($MgAl_2O_4$) [1], high alumina cement ($CaAl_2O_4$, $Ca_3Al_2O_6$) [2], pigments and glazes ($CoAl_2O_4$) [3, 4], catalysts ($ZnAl_2O_4$, $CuAl_2O_4$) [5, 6], TV phosphors and in fluorescent lamps ($CaAl_{12}O_{19}:Ce^{3+}$, $CeMgAl_{11}O_{19}$) [7, 8]. The preparation of these metal aluminates usually involves the solid-state reaction of the corresponding metal oxides with Al_2O_3 at high temperatures, e.g. MgO–Al_2O_3 (1560° C) [9], ZnO–Al_2O_3 (1400° C) [10] and NiO–Al_2O_3 (1050° C) [11]. Preparation of fine-particle metal aluminates can be achieved by the decomposition of co-precipitated oxalates [12], sulphates [13], nitrates [14] or by sol–gel [15] and spray decomposition [16] processes. However, most of these methods are involved, requiring high temperatures and long periods. We describe here the preparation of fine-particle metal aluminates by a low-temperature initiated combustion process [17] developed earlier for the preparation of α-alumina, ruby and related oxide materials. The process makes use of the heat energy liberated by the redox exothermic reaction at 500 or 350° C between metal nitrates (oxidizers) and urea or carbohydrazide (fuels), respectively. The process is safe, instantaneous and energy-saving.

2. Experimental procedure

Stoichiometric compositions of the metal nitrates (oxidizers) and urea or carbohydrazide (fuels) were calculated using the total oxidizing and reducing valencies of the components which serve as numerical coefficients for stoichiometric balance, so that the equivalent ratio ϕ_e is unity and the energy released by the combustion is at a maximum [18].

2.1. Synthesis of metal aluminates using metal nitrate–aluminium nitrate–urea mixtures

In a typical experiment, $Al(NO_3)_3 \cdot 9H_2O$ (20 g) and $Sr(NO_3)_2 \cdot 4H_2O$ (7.56 g) were dissolved in a minimum quantity of water along with urea (10.7 g) in a cylindrical Pyrex dish (100 mm diameter × 50 mm height) of approximately 300 ml capacity. The dish containing the solution was introduced into a muffle furnace (l = 28 cm, b = 17 cm and h = 9 cm) maintained at 500 ± 10° C. Initially, the solution boils and undergoes dehydration followed by decomposition with the evolution of large amounts of gases (oxides of nitrogen and ammonia). The mixture then froths and swells, forming a foam which ruptures with a flame and glows to incandescence. During incandescence the foam further swells to the capacity of the container. The flame temperature as measured by an optical pyrometer is around 1600 ± 20° C. The product of combustion is a voluminous and foamy $SrAl_2O_4$ (weight 5.48 g, 100% yield) with a foam density of 0.01 g cm^{-3} (Fig. 1). The whole process is over in less than 5 min.

The compositions of the mixtures used for the combustion synthesis of other metal aluminates, MAl_2O_4 where M = Mg, Ca, Ba and Zn, and tricalcium aluminate, calcium hexa-aluminate and magnesium cerium aluminate, are given in Table I. Note that $BaAl_2O_4$ was prepared using a ground mixture of $Ba(NO_3)_2$, $Al(NO_3)_3 \cdot 9H_2O$ and urea owing to the low solubility of $Ba(NO_3)_2$ in water.

2.2. Synthesis of metal aluminates using metal nitrate–aluminium nitrate–carbohydrazide mixtures

The fuel carbohydrazide (NH_2–NH–CO–NH–NH_2) was prepared by refluxing diethyl carbonate with $N_2H_4 \cdot H_2O$ in the mole ratio 1:2 for 3 h [19]. The crystalline product (m.p. 154° C) was isolated after reducing the mother liquor to half of its volume by distillation and cooling.

In a typical experiment, $Ni(NO_3)_2 \cdot 6H_2O$ (3.87 g) and $Al(NO_3)_3 \cdot 9H_2O$ (10 g) were dissolved in a minimum quantity of water along with carbohydrazide (4.5 g) in a cylindrical Pyrex dish (150 mm diameter × 75 mm height). The dish containing the solution

0022–2461/90 $03.00 + .12

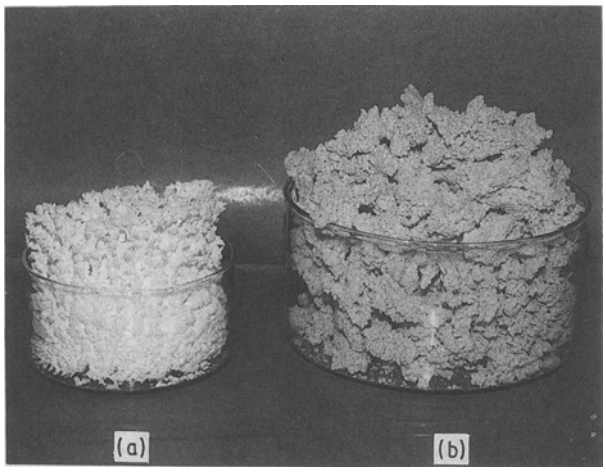

Figure 1 (a) $SrAl_2O_4$ foam as formed (weight 5.48 g, volume 300 cm^3) (urea process), (b) $NiAl_2O_4$ as formed (weight 2.35 g, volume 1200 cm^3) (carbohydrazide process).

was heated on a hotplate (350° C). Initially, the solution boils and undergoes dehydration followed by decomposition, generating traces of NO_2 and other combustible such as NH_3 and N_2H_4. The mixture then ignites, leading to smooth deflagration with enormous swelling, producing a light blue coloured foam. The product of combustion is a voluminous and foamy $NiAl_2O_4$ (weight 2.35 g, 100% yield) with a foam density of 1.96×10^{-3} g cm^{-3} (Fig. 1). The compositions of the mixtures used for the combustion synthesis of other metal aluminates, MAl_2O_4 where M = Mn, Co and Cu, are given in table II.

2.3. Physical measurements

X-ray powder diffraction patterns of the combustion products were recorded using a Philips X-ray diffractometer model PW 1050/70 using a Cu$K\alpha$ radiation with a nickel filter. The powder densities of all the oxide materials were measured employing a pycnometer and xylene medium. The BET surface area measurements were made by nitrogen adsorption employing a Micromeritics AccuSorb 2100E instrument. Particle size analysis was done using a Micron Photo Sizer model SKC 2000, based on the light scattering principle and employing a sedimentation technique. The macrostructure and morphology of the metal aluminates were studied using a Cambridge Stereoscan model S-150 scanning electron microscope (SEM) and a Philips EM 301 transmission electron microscope (TEM) operated at 100 kV. The excitation and emission spectra of Cr^{3+}- and Ce^{3+}-doped metal aluminates were recorded using a Hitachi 650-60 fluorescence spectrophotometer. The diffuse reflectance UV–visible spectrum of $NiAl_2O_4$ was recorded using a Shimadzu spectrophotometer model UV-240 with $BaSO_4$ as standard.

3. Results and discussion

3.1. Preparation and characterization of fine-particle metal aluminates

The combustion process [17] developed earlier for the preparation of high-temperature ceramic oxides like α-Al_2O_3, ruby and $LaAlO_3$ has now been extended to the preparation of fine-particle metal aluminates, MAl_2O_4 where M = Mg, Ca, Ba, Sr and Zn, $Ca_3Al_2O_6$, $CaAl_{12}O_{19}$ and $MgCeAl_{11}O_{19}$. These metal aluminates were obtained by the combustion of corresponding metal nitrate–aluminium nitrate–urea mixtures as described in Section 2.1. The formation of single-phase products was confirmed by their characteristic X-ray powder diffraction patterns. Typical X-ray diffraction (XRD) patterns of the as-prepared $CaAl_2O_4$, $Ca_3Al_2O_6$ and $ZnAl_2O_4$ are shown in Fig. 2. The lattice constants calculated from the XRD patterns are in good agreement with the literature [20], e.g. for $ZnAl_2O_4$ a = 0.80682 nm and for $MgAl_2O_4$ a = 0.81153 nm. It may be noted that metal aluminates with different structures such as $CaAl_2O_4$, $Ca_3Al_2O_6$, $CaAl_{12}O_{19}$ and $MgCeAl_{11}O_{19}$ could be prepared by just changing the metal nitrate–aluminium nitrate ratio in the combustion mixture.

Although the combustion process using urea as a fuel was successful in the preparation of these refractory metal aluminates, it could not be employed for the preparation of certain other transition metal aluminates, MAl_2O_4 where M = Mn, Co, Ni and Cu, due to their low thermal stability. For example, $CuAl_2O_4$ is known [21] to decompose above 1000° C to $CuAlO_2$. Therefore an alternate redox mixture with

TABLE I Compositions of the combustion mixtures and the properties of their combustion products

No.	Composition of the combustion mixtures*	Product†	Powder density (g cm^{-3})	Surface area (BET) (m^2 g^{-1})	Particle size (from surface area) (μm)	50% average agglomerate size (from sedimentation) (μm)
1.	$Mg(NO_3)_2 \cdot 6H_2O$ (6.83 g) + A	$MgAl_2O_4$	3.00	21.80	0.10	5.2
2.	$Ca(NO_3)_2 \cdot 4H_2O$ (6.29 g) + A	$CaAl_2O_4$ (CA)	2.48	1.25	1.92	4.1
3.	$Sr(NO_3)_2 \cdot 4H_2O$ (7.56 g) + A	$SrAl_2O_4$	2.88	2.41	0.86	5.7
4.	$Ba(NO_3)_2$ (6.96 g) + A	$BaAl_2O_4$	3.20	2.01	0.93	5.8
5.	$Zn(NO_3)_2 \cdot 6H_2O$ (7.93 g) + A	$ZnAl_2O_4$	3.60	8.70	0.19	5.4
6.	$Ca(NO_3)_2 \cdot 4H_2O$ (18.88 g) + B + urea (16.01 g)	$Ca_3Al_2O_6$ (C_3A)	2.50	1.40	1.71	6.2
7.	$Ca(NO_3)_2 \cdot 4H_2O$ (1.05 g) + B + urea (8.45 g)	$CaAl_{12}O_{19}$ (CA_6)	2.85	8.34	0.25	4.1
8.	$Mg(NO_3)_2 \cdot 6H_2O$ (1.24 g) + B + $Ce(NO_3)_3 \cdot 6H_2O$ (2.1 g) + urea (9.22 g)	$MgCeAl_{11}O_{19}$	3.71	20.20	0.08	3.2

*A = $Al(NO_3)_3 \cdot 9H_2O$ (20 g) + urea (10.7 g); B = $Al(NO_3)_3 \cdot 9H_2O$ (20 g).
†Obtained at 500° C under normal atmospheric pressure.

TABLE II Compositions of the combustion mixtures and the properties of their combustion products

No.	Composition of the combustion mixture*	Product† (colour)	Powder density ($g\,cm^{-3}$)	Lattice constant, a (nm)		Crystallite size (from XRD) (nm)	Surface area (BET) ($m^2\,g^{-1}$)	Particle size (from surface area) (nm)	50% average agglomerate size (from sedimentation) (μm)
				Calculated	Reported				
1.	$Mn(NO_3)_2 \cdot 4H_2O$ (3.345 g) + A	$MnAl_2O_4$ (Brown)	2.629	8.3075	8.2580	10.81	43.2	52.82	2.70
2.	$Co(NO_3)_2 \cdot 6H_2O$ (3.879 g) + A	$CoAl_2O_4$ (Thenard's blue)	3.262	8.1370	8.1030	11.82	58.3	31.55	2.15
3.	$Ni(NO_3)_2 \cdot 6H_2O$ (3.876 g) + A	$NiAl_2O_4$ (sky-blue)	3.091	8.0756	8.0458	12.30	83.4	22.48	1.24
4.	$Cu(NO_3)_2 \cdot 3H_2O$ (3.220 g) + A	$CuAl_2O_4$ (Greenish brown)	3.710	8.1204	8.0800	13.49	59.8	27.08	1.90

*A = $Al(NO_3)_3 \cdot 9H_2O$ (10 g) + carbohydrazide (4.5 g).
†Obtained at 350° C (hotplate) under normal atmospheric pressure.

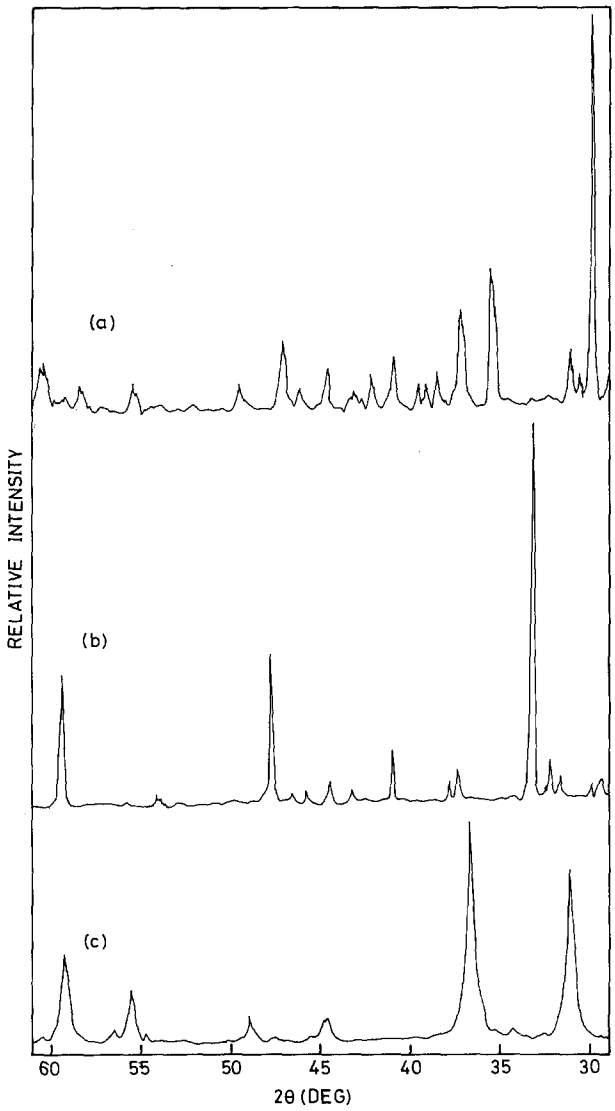

Figure 2 X-ray powder diffraction patterns of (a) $CaAl_2O_4$, (b) $Ca_3Al_2O_6$ and (c) $ZnAl_2O_4$.

low exothermicity (< 1000° C) was required. During the course of our search for such a redox mixture, we have come across a derivative of urea (NH_2–CO–NH_2), namely carbohydrazide (NH_2–NH–CO–NH–NH_2) which is reported [22] to be formed by the reaction of urea with hydrazine (NH_2–NH_2). This fuel, being richer in nitrogen than urea, decomposes at lower temperatures (300° C) to yield large amounts of cold gaseous products like N_2, H_2O, and NH_3 and thereby it could reduce the exothermicity of the combustion process. It was gratifying that the combustion of metal nitrate–aluminium nitrate–carbohydrazide mixtures yielded foamy and voluminous metal aluminates, MAl_2O_4 where M = Mn, Co, Ni and Cu. These transition metal aluminates were prepared as described in Section 2.2.

A typical XRD pattern of the as-prepared $NiAl_2O_4$ is shown in Fig. 3. It can be seen from the XRD pattern that the peaks are quite broad and indicate the fine nature of the product. The crystallite sizes of these metal aluminates calculated from the XRD line-broadening using Scherrer's equation [23] are in the range 10 to 15 nm (Table II). The lattice constants (Table II) calculated from the XRD patterns of these metal aluminates are in good agreement with the literature [20]. The electronic spectrum of the blue-coloured $NiAl_2O_4$ is shown in Fig. 4. The absorption maxima at 378, 600 and 638 nm correspond to the transitions $^3A_{2g} \rightarrow {}^3T_{2g}$, $^3A_{2g} \rightarrow {}^3T_{1g}$ (F) and $^3A_{2g} \rightarrow {}^3T_{1g}$ (P), respectively [24].

The properties like density, particle size and surface area of all the combustion-synthesized metal aluminates are summarized in Table I and II. It can be seen that the surface areas of the metal aluminates obtained from the combustion of metal nitrate–aluminium nitrate–urea mixtures are low (1 to 20 $m^2 g^{-1}$), whereas those of the metal aluminates prepared from the carbohydrazide process are quite high (45 to 85 $m^2 g^{-1}$). A possible explanation for this wide variation in the surface area values could be attributed to the higher exothermic combustion reaction of metal nitrate–urea mixtures (flame temperature of ~ 1600° C) compared to the metal nitrate–carbohydrazide mixtures (flame temperature of ~ 1000° C). This fact is also reflected in the foam volumes (Fig. 1) and densities as well as the particle size distributions of the different metal aluminates (Tables I and II). The particle size distributions of

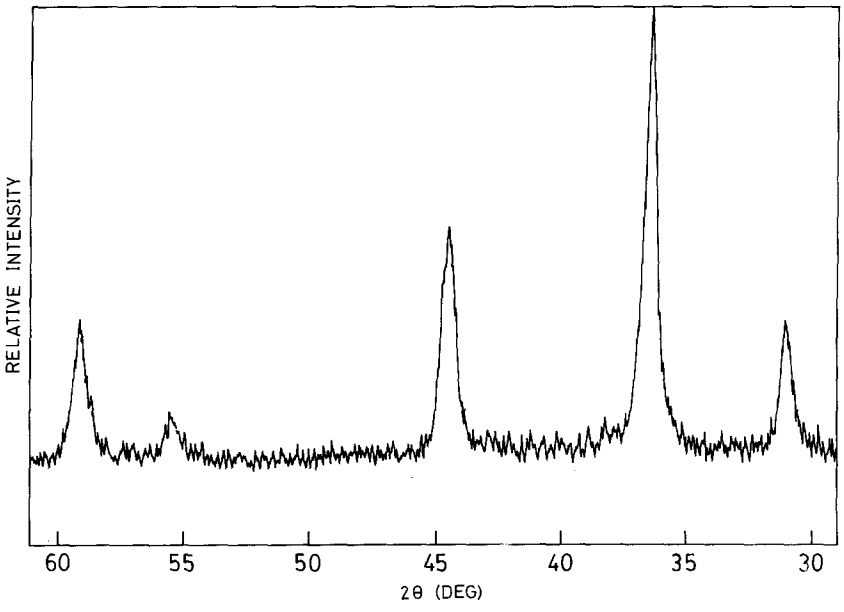

Figure 3 X-ray powder diffraction pattern of $NiAl_2O_4$.

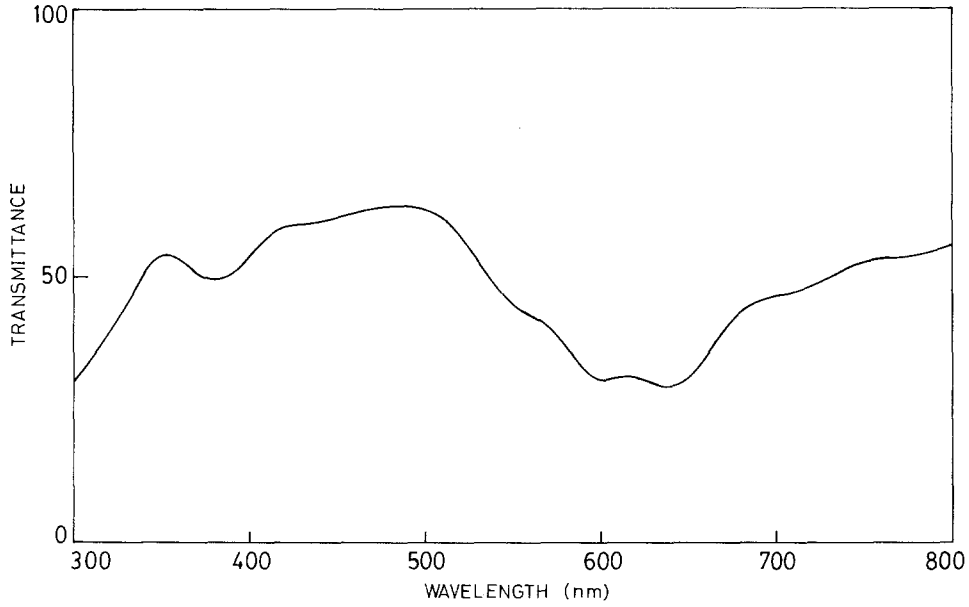

Figure 4 UV–visible reflectance spectrum of $NiAl_2O_4$.

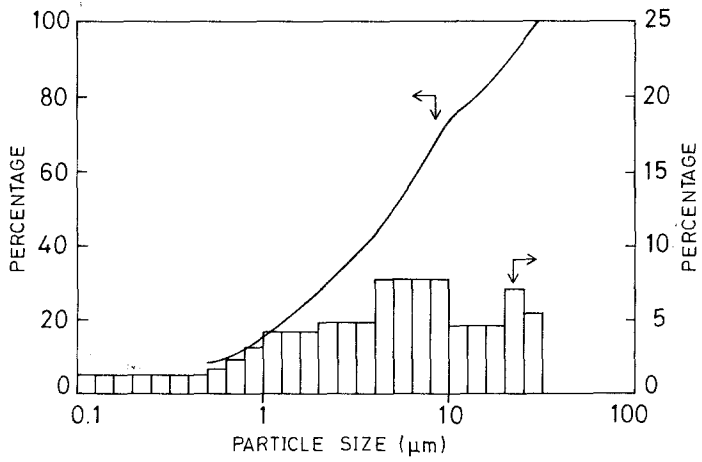

Figure 5 Particle size distribution of $ZnAl_2O_4$ (urea process).

$ZnAl_2O_4$ (urea process) and $NiAl_2O_4$ (carbohydrazide process) are given in Figs 5 and 6, respectively, for comparison. Average agglomerate sizes of the metal aluminates from urea and carbohydrazide processes are in the range 3 to 6 μm and 1 to 2.5 μm, respectively. It should be emphasized that the particle size distributions of metal aluminates obtained by the carbohydrazide process have a narrow range which does not exceed 10 μm (Fig. 6). The values of the powder densities of these metal aluminates (Tables I and III) correspond nearly to 60 to 80% of the theoretical density. The tap densities of these aluminates are low, e.g. 0.10 g cm^{-3} for $SrAl_2O_4$ (urea process) and 0.02 g cm^{-3} for $NiAl_2O_4$ (carbohydrazide process) and they reflect the fluffy and fine nature of these products.

SEM micrographs of $MgAl_2O_4$ (urea process) and $NiAl_2O_4$ (carbohydrazide process) foams are shown in Fig. 7. The foamy macrostructure of the aluminates reflects the inherent nature of the combustion process. The surfaces of the foams show a lot of cracks and

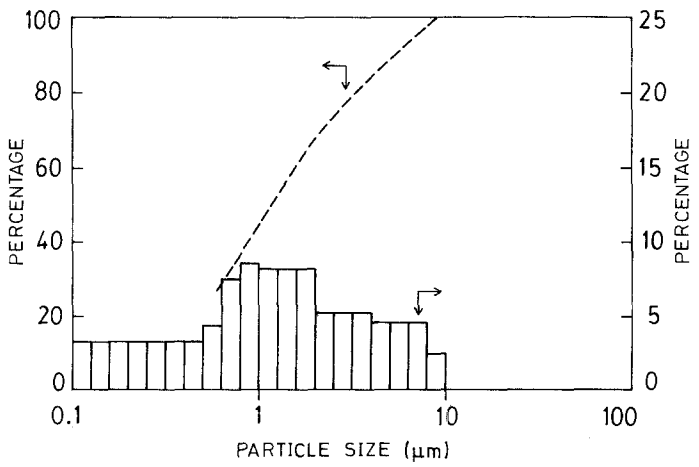

Figure 6 Particle size distribution of $NiAl_2O_4$ (carbohydrazide process).

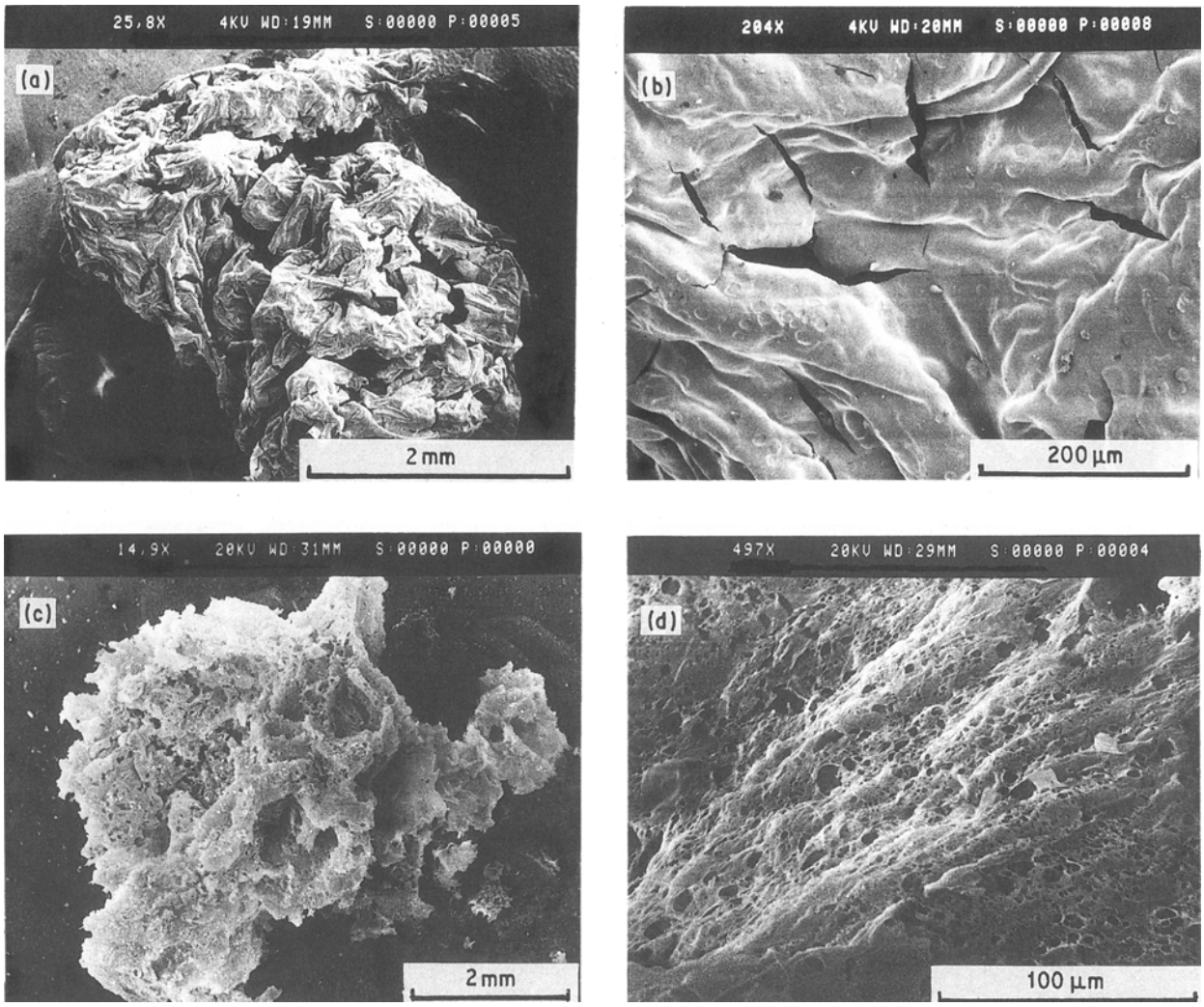

Figure 7 SEM micrographs: (a) $MgAl_2O_4$ foam (urea process), (b) surface of the $MgAl_2O_4$ foam, (c) $NiAl_2O_4$ foam (carbohydrazide process), (d) surface of $NiAl_2O_4$ foam.

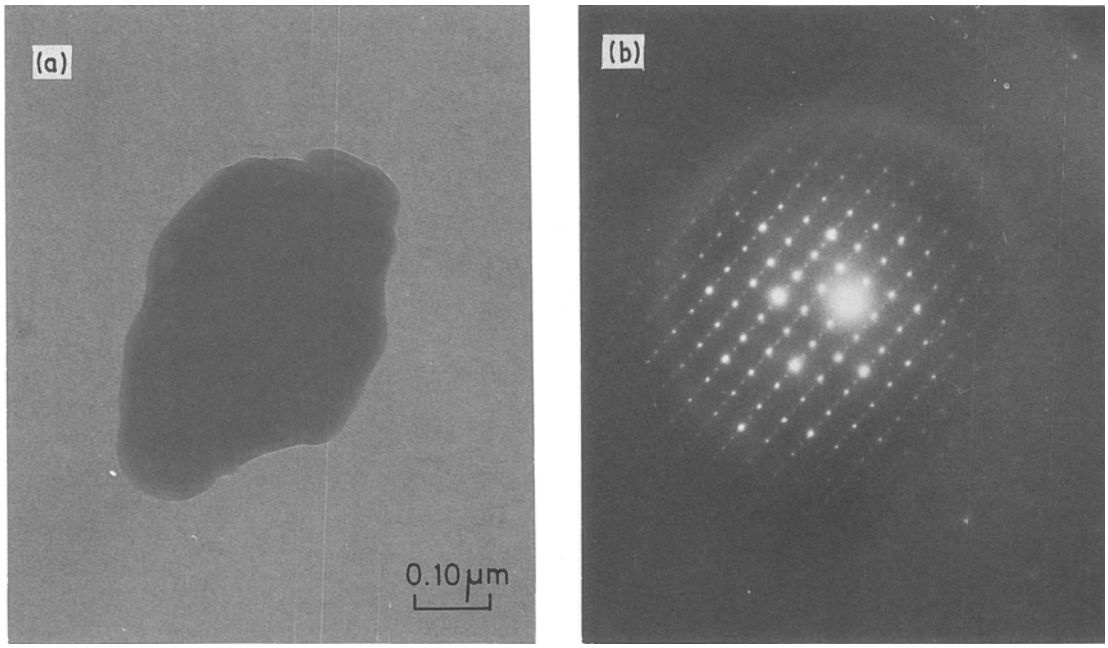

Figure 8 TEM micrographs: (a) $CaAl_2O_4$ particle, (b) electron diffraction of $CaAl_2O_4$, (c) fibrous $NiAl_2O_4$ matrix, (d) polycrystalline electron diffraction of $NiAl_2O_4$.

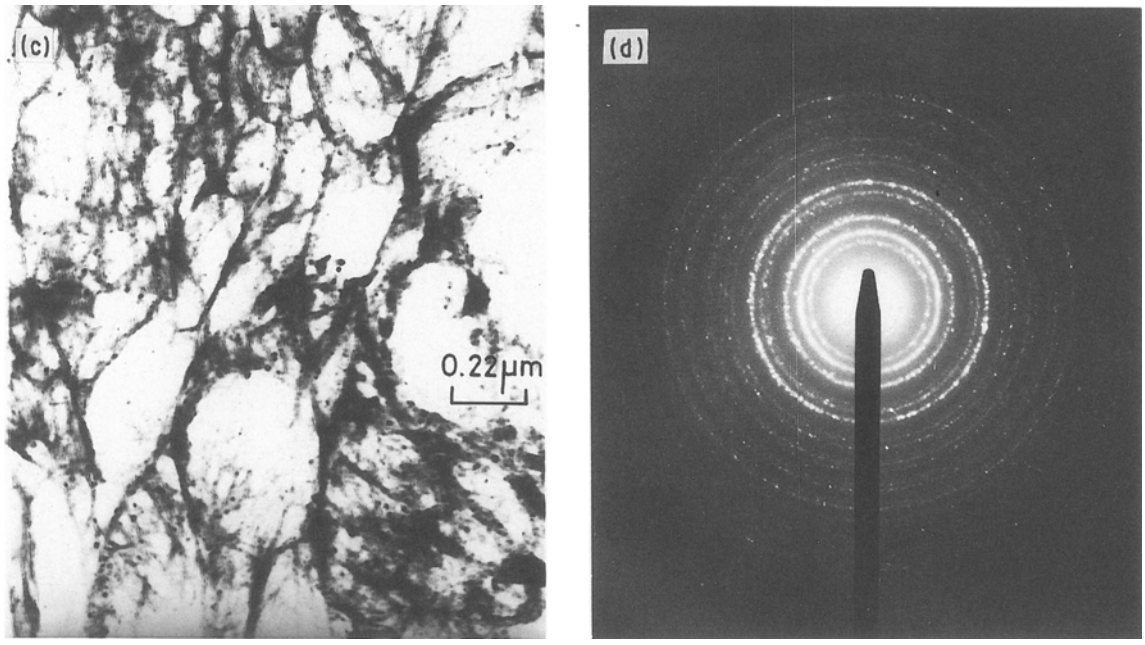

Figure 8 continued

pores formed by the escaping gases during combustion. It can be seen that the $NiAl_2O_4$ foam (Fig. 7d) has a more fibrous structure compared to $MgAl_2O_4$ (Fig. 7b). The TEM micrographs of $CaAl_2O_4$ (Fig. 8a) and $NiAl_2O_4$ (Fig. 8c) particles show their morphology. The electron diffraction patterns of $CaAl_2O_4$ and $NiAl_2O_4$ (Figs 8b and d) show their difference in crystallinity. The particle sizes of the aluminates calculated from the TEM observations are in the range 0.1 to 0.8 μm. These low values compared to the values obtained from the particle size analysis could be attributed to the strong tendency of these fine particles to cluster into weakly bound agglomerates through a small degree of ceramic bonding [25].

3.2. Preparation and characterization of fluorescent metal aluminates

It was thought worth while to prepare Cr^{3+}-doped spinel, $MgAl_2O_4$, similar to the preparation of ruby (Cr^{3+}-doped α-Al_2O_3) powder by the combustion process [17]. The reaction mixture containing $Cr(NO_3)_3 \cdot 6H_2O$ (0.0286 g) (equivalent to 0.2 wt % Cr_2O_3 in Al_2O_3), $Mg(NO_3)_2 \cdot 6H_2O$ (6.83 g), $Al(NO_3)_3 \cdot 9H_2O$ (20 g) and urea (10.7 g), when heated at 500° C gave a pale pink foamy material after combustion. It was identified as Cr^{3+}-doped $MgAl_2O_4$ by its characteristic fluorescence spectra [26] (Figs 9 and 10). It may be noted that the emission at 687 nm is due to the Cr^{3+} substituted in O_h sites of Al^{3+} ions in

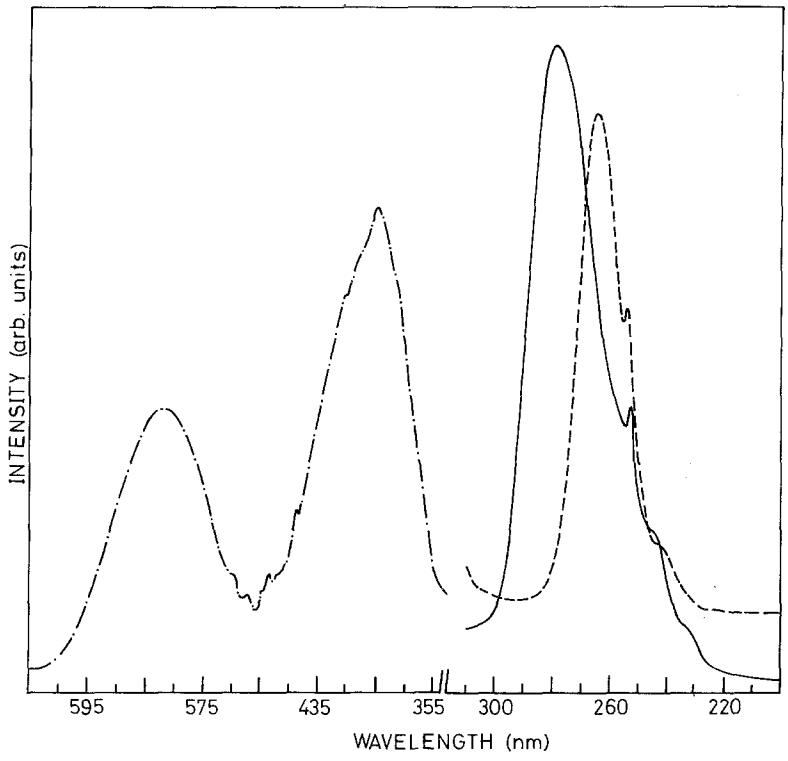

Figure 9 Excitation spectra of the luminescence in (– – –) 0.05 wt % $Cr^{3+}/MgAl_2O_4$, (– · –) $CaAl_{12}O_{19}$:0.14Ce^{3+} and (——) $MgCeAl_{11}O_{19}$.

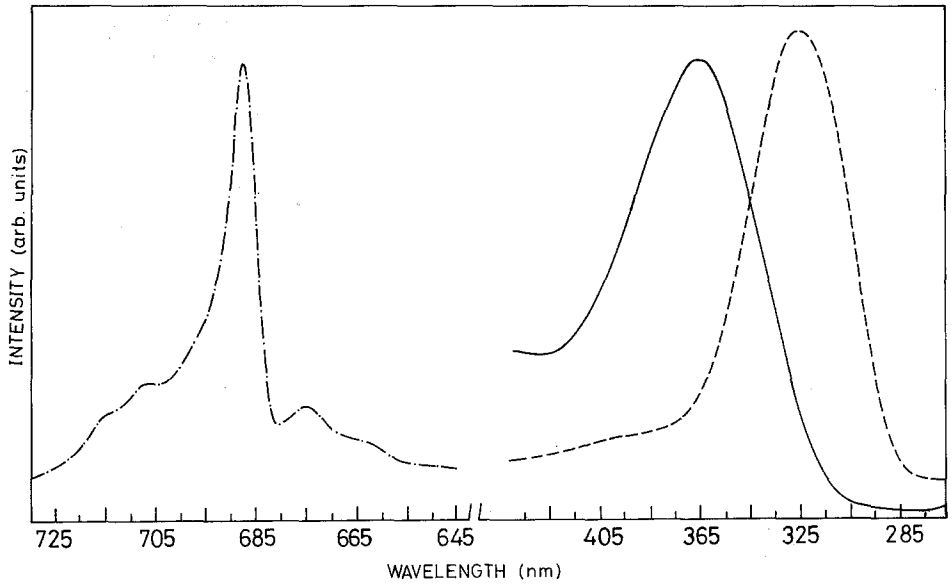

Figure 10 Emission spectra of the luminescence in (- - -) 0.05 wt % $Cr^{3+}/MgAl_2O_4$, (— —) $CaAl_{12}O_{19}$:0.14Ce^{3+} and (——) $MgCeAl_{11}O_{19}$.

the $MgAl_2O_4$ lattice. Thus, the combustion process not only yields a homogeneous and stoichiometric product but also helps in substituting Cr^{3+} ions for Al^{3+} ions due to the high *in situ* temperatures.

It has also been possible to obtain Ce^{3+}-doped $CaAl_{12}O_{19}$ and $CeMgAl_{11}O_{19}$ by this process. The characteristic fluorescence spectra of the as-prepared $CaAl_{12}O_{19}$:0.14Ce^{3+} and $CeMgAl_{11}O_{19}$, are shown in Figs 9 and 10. The excitation wavelengths of $CaAl_{12}O_{19}$:0.14Ce^{3+} and $CeMgAl_{11}O_{19}$ are seen at 265 and 281 nm, respectively. The characteristic emission wavelengths of $CaAl_{12}O_{19}$:0.14Ce^{3+} and $CeMgAl_{11}O_{19}$ are observed at 325 and 370 nm, respectively. These results of the fluorescence spectral studies are in good agreement with the literature [7, 27].

4. Conclusions

Low-temperature initiated gas-producing exothermic reactions involving metal nitrate–urea/carbohydrazide redox mixtures have been successfully employed in the preparation of fine-particle metal aluminates. Formation of the different metal aluminates appears to be controlled by the exothermicity of the redox reaction, which in turn is dependent on the fuel–oxidizer combination. This combustion process is also useful in the preparation of metal aluminates with desired impurities for applications as lasers and phosphors.

References

1. W. H. GITZEN, "Alumina as a Ceramic Material" (American Ceramic Society, Columbus, Ohio, 1970) p. 141.
2. A. NEVILLE, "High Alumina Cement" (Wiley, New York, 1975) p. 1.
3. Y. OOBA, T. KANO, M. HAYASHI, H. TAKADA, S. KANDA, S. EGUCHI, S. ORMATOI and T. HATSCMI, *Jpn. Kokai. Tokkyo Koho.* (1978) 76, 183. (*Chem. Abstr.* **90** (1979) P96532g).
4. S. PARK, *Yoop Hoe Chi* **15** (2) (1978) 66 (in Korean) (*Chem. Abstr.* **90** (1979) 59811b).
5. G. P. CHERNYUK, Zh. Prikl. Khim (Leningrad) **54** (6) (1981) 1384 (in Russian) (*Chem. Abstr.* **95** (1981) 96919s).
6. H. PAETWO and L. RIEKERT, *Act. Phys. Chem.* **24** (1-2) (1978) 245.
7. A. L. N. STEVELS, *J. Electrochem. Soc.* 125 (4) (1978) 588.
8. P. C. SCHOLTEN and R. EIJNTHOVEN, European Patent Application (1985) EP 140,448. (*Chem. Abstr.* **103** (1985) P 30124f).
9. R. C. ROSSI and A. M. FULRATH, *J. Amer. Ceram. Soc.* **46** (1963) 145.
10. M. R. ANSEAV, F. CAMBILER, C. LE BLUD, *J. Mater. Sci. Lett.* **16** (1981) 1121.
11. S. MOON, *Hwahak. Honghak* **12** (1) (1978) 33 (in Korean) (*Chem. Abstr.* **81** (1974) 30185d).
12. H. SCHUMANN, N. CONRAD and R. SCHRADEV, *Silikattechnik* **23** (4) (1972) 119 (in German) (*Chem. Abstr.* **83** (1975) 197340d).
13. J. G. M. DE LAU, *Amer. Ceram. Soc. Bull* **49** (6) (1970) 572.
14. D. R. MESSIER and G. E. GAZZA, *ibid.* **51** (9) (1972) 692.
15. A. SEN and D. CHAKRAVORTY, in "Advances in Solid State Chemistry, edited by C. N. R. Rao (INSA, New Delhi, 1986) p. 159.
16. B. JOWER, J. JUHASZ and G. SZABO ZOLTAN, *Magy. Kem. Foly* **89** (10) (1983) 450 (in Hungarian) (*Chem. Abstr.* **100** (1984) 28804×).
17. J. J. KINGSLEY and K. C. PATIL, *Mater. Lett.* **6** (11, 12) (1988) 427.
18. S. R. JAIN, K. C. ADIGA and V. R. PAI VERNEKAR, *Combust. Flame* **40** (1981) 71.
19. E. B. MOHR, J. J. BREZINSKI and L. F. AUDRIETH, in "Inorganic Synthesis", Vol. 4, edited by J. C. Bailer Jr (McGraw-Hill, New York, 1953) p. 32.
20. Powder Diffraction File, Inorganic Vol. PDIS-10 (Joint Committee on Diffraction Standards. Pennsylvania, 1967).
21. T. TSUCHIDA, R. FURCUCHI, T. SUKEGAWA, M. FURUDATE and T. ISHII. *Thermochim. Acta* **78** (1-3) (1984) 71.
22. W. ENGEL, Report 6/70 (German Institute for Chemical Propulsion and Explosives, ICT, Burghausen, W. Germany) (in German).
23. H. KLUG and L. ALEXANDER, "X-ray Diffraction Procedures", (Wiley, New York, 1962) p. 491.
24. C. J. BALLHAUSEN, "Introduction to Ligand Field Theory" (McGraw-Hill, New York, 1962) p. 261.
25. D. A. HARRISON, R. STEVENS and S. J. MILNE, *J. Mater. Sci. Lett.* **6** (1987) 673.
26. D. L. WOOD, G. F. IMBOSCH, R. M. MACFARLANE, P. KISLUIK and D. M. LARKIN, *J. Chem. Phys.* **48** (11) (1968) 5255.
27. J. M. P. J. VERSTEGEN, J. L. SOMMERDIJK and J. G. VERRIET, *J. Luminesc.* **6** (1973) 425.

Received 9 December 1988
and accepted 11 May 1989